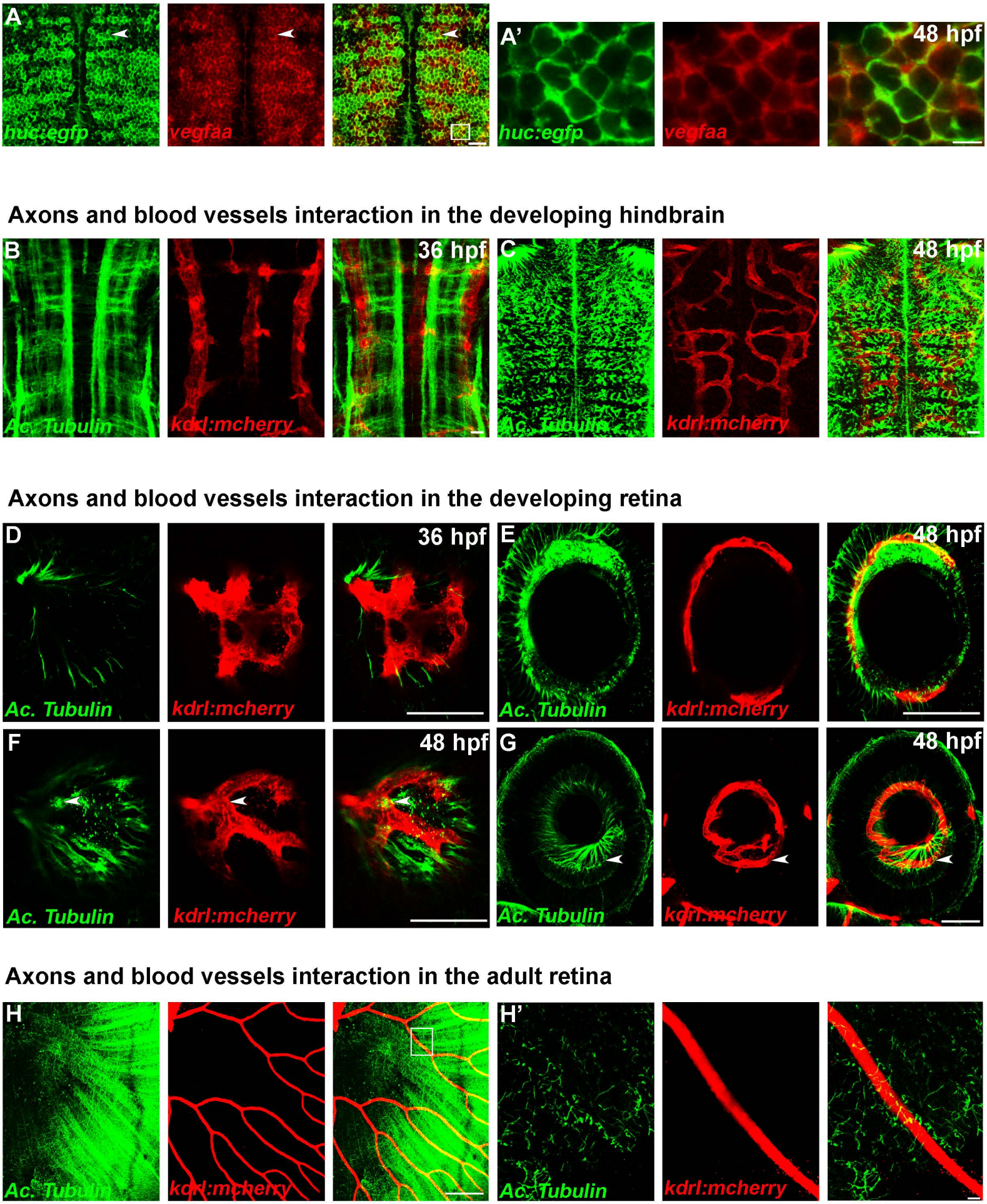
Zebrafish neuronal *vegfa* expression in the developing hindbrain
A
huc:egfp
vegfaa
A'
huc:egfp
vegfaa
48 hpf
Axons and blood vessels interaction in the developing hindbrain
B
Ac. Tubulin
kdrl:mcherry
36 hpf
C
Ac. Tubulin
kdrl:mcherry
48 hpf
Axons and blood vessels interaction in the developing retina
D
Ac. Tubulin
kdrl:mcherry
36 hpf
E
Ac. Tubulin
kdrl:mcherry
48 hpf
F
Ac. Tubulin
kdrl:mcherry
48 hpf
G
Ac. Tubulin
kdrl:mcherry
48 hpf
Axons and blood vessels interaction in the adult retina
H
Ac. Tubulin
kdrl:mcherry
H'
Ac. Tubulin
kdrl:mcherry

Figure S1

Supplemental Figure 1: Neurons expressing VEGF-A are closely associated with blood vessels (related to Figure 1)

(A) Confocal section of double *in situ*/immunolabelling with *vegfaa* and EGFP in the hindbrain of *Tg(huc:egfp)* line at 48 hpf shows neuronal expression of *vegfa* in the zebrafish brain. Close up of *vegfaa* expression in the hindbrain (A'). **(B, C)** Confocal section of double immunolabelling showing the physical interaction/close proximity between axons (Acetyl Tubulin, green) and blood vessels (red) in *Tg(kdrl:mCherry)* hindbrain at 36 and 48 hpf. **(D-H)** Confocal section of double immunolabelling showing the physical interaction/close proximity between axons (Acetyl Tubulin, green) and blood vessels (red) in *Tg(kdrl:mCherry)* retina at 36 hpf, 48 hpf or in the adult retina. Close up on a blood vessel in the adult retina (H'). Arrowheads show co-localization. Dorsal view of the brain with anterior up. Lateral view of the retina. Scale bars: 100 μm (A and D-H) or 10 μm (A', B, C and H').

A zebrafish NSCs
in the developing hindbrain

B zebrafish NSCs in the adult
ventricular zone of the telencephalon

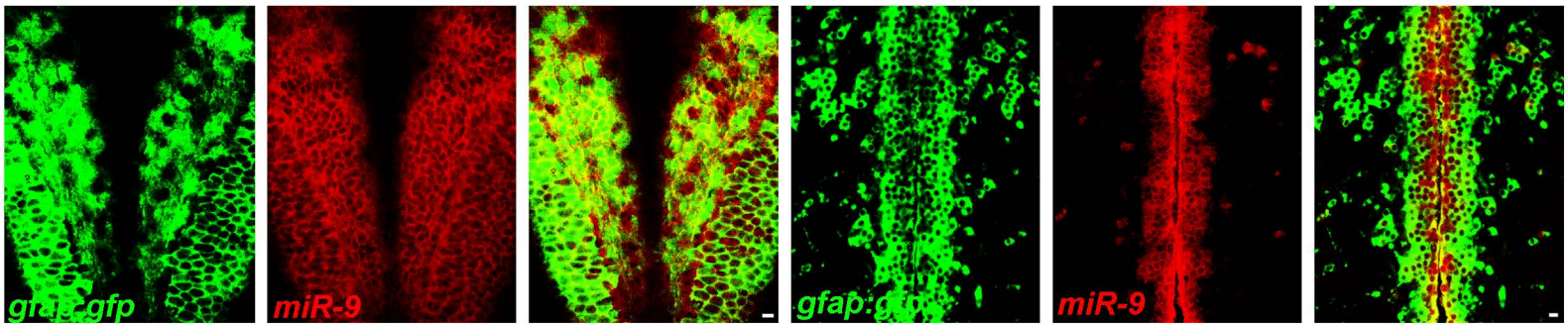

C Dynamic of *miR-9* expression during development

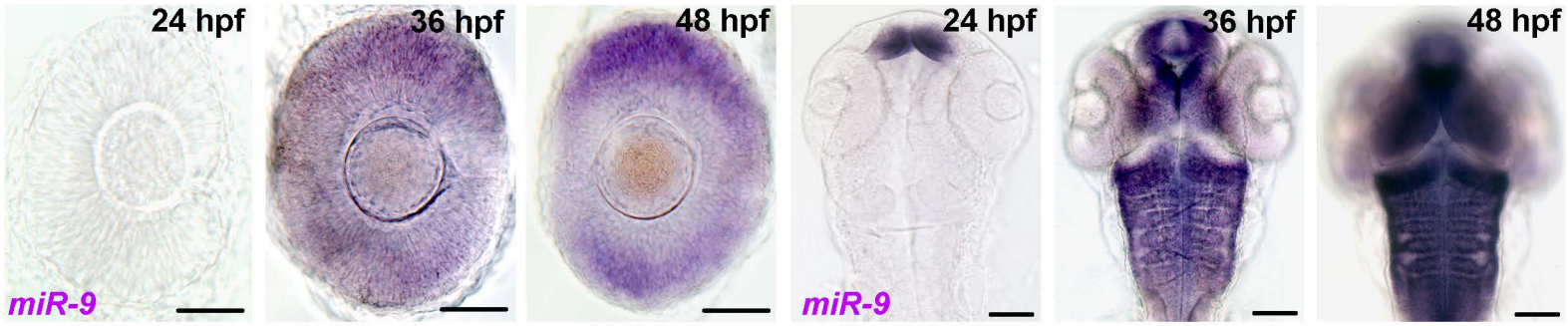

Figure S2

Supplemental Figure 2: miR-9 expression in NSCs in the zebrafish brain (related to Figure 1)

(A, B) Confocal section of double in situ/immunolabelling showing extensive overlap in the expression of endogenous *miR-9* and EGFP protein in hindbrain at 72 hpf or in the ventricular zone of the adult zebrafish telencephalon in the *Tg(gfap:gal4)*, *Tg(uas:egfp)* line, revealing miR-9 expression in embryonic and adult NSCs. **(C)** Whole-mount in situ hybridization against *miR-9* showing the time course of *miR-9* expression in the developing embryo at 24, 36 and 48 hpf. Dorsal view of the brain with anterior up. Lateral view of the retina. Scale bars: 10 μm (A, B) or 100 μm (C).

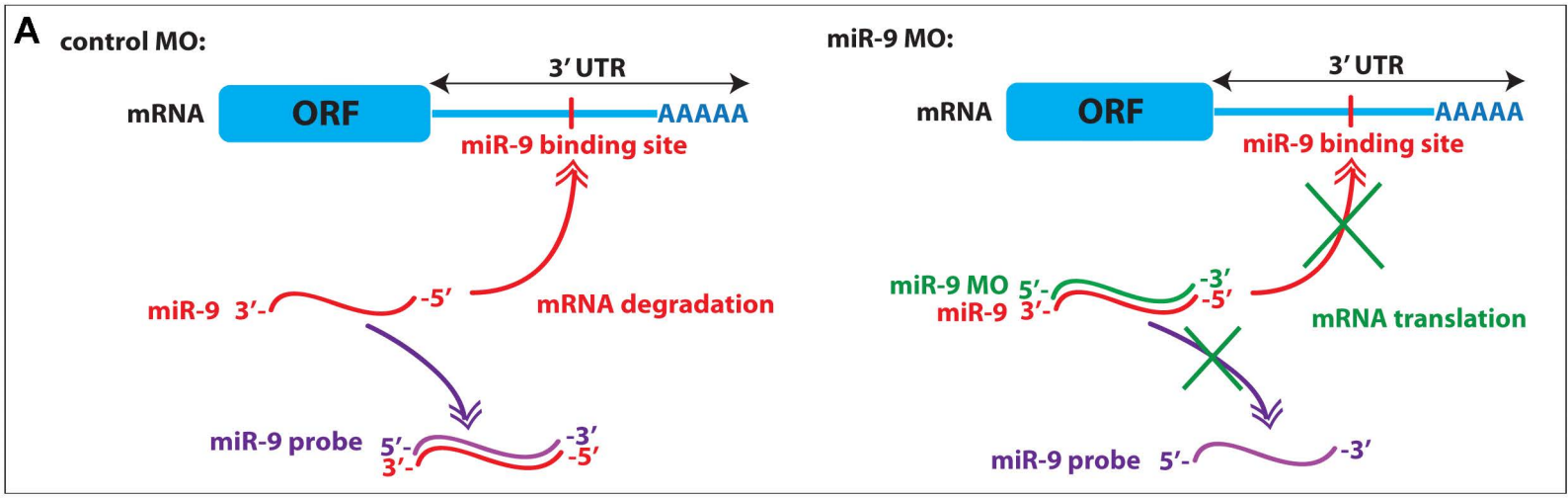
A
control MO:
mRNA
ORF
3′ UTR
AAAAA
miR-9 binding site
miR-9 3′-
-5′
mRNA degradation
miR-9 probe
5′-
3′-
-3′
-5′
miR-9 MO:
miR-9 MO 5′-
miR-9 3′-
-3′
-5′
mRNA translation
miR-9 probe 5′-
-3′

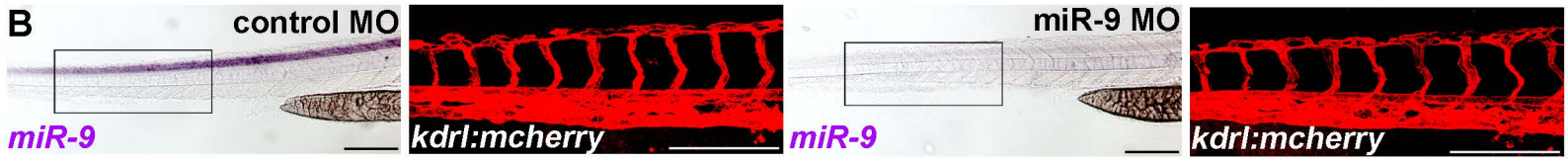
B
control MO
miR-9
kdrl:mcherry
miR-9 MO
miR-9
kdrl:mcherry


C
control MO
Box1
Box2
miR-9 MO
Box1
Hyloid vasculature
Box3

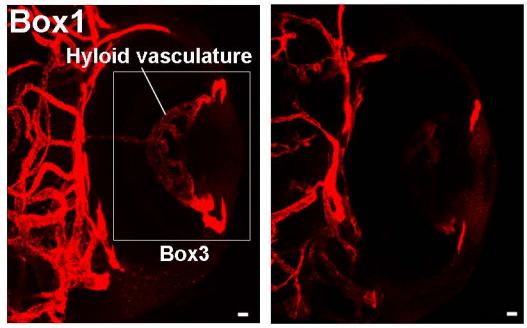
Box3
kdrl:mcherry

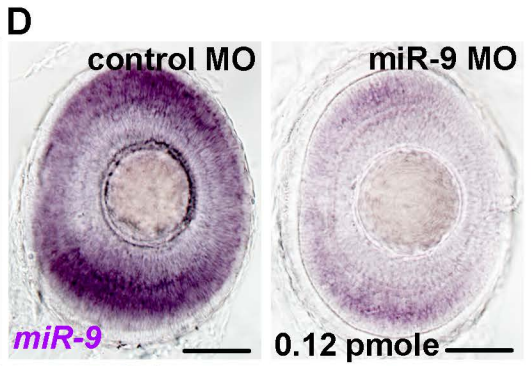
D
control MO
miR-9
miR-9 MO
0.12 pmole
miR-9 MO
0.5 pmole
miR-9 MO
2 pmole


group 1
group 2
group 3
group 4
kdrl:mcherry

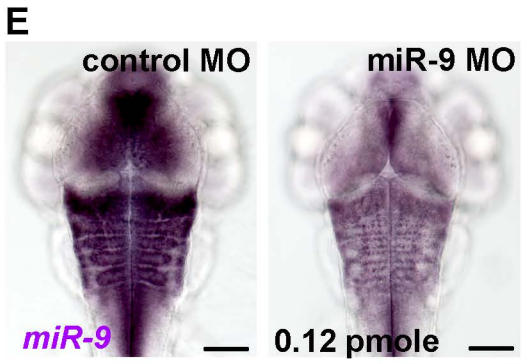
E
control MO
miR-9
miR-9 MO
0.12 pmole
miR-9 MO
0.5 pmole
miR-9 MO
2 pmole

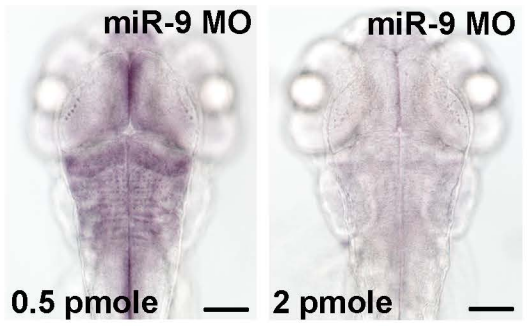
Box2
PCS
PHBC
CtA
BA
control MO
miR-9 MO
0.12 pmole
miR-9 MO
0.5 pmole
miR-9 MO
2 pmole

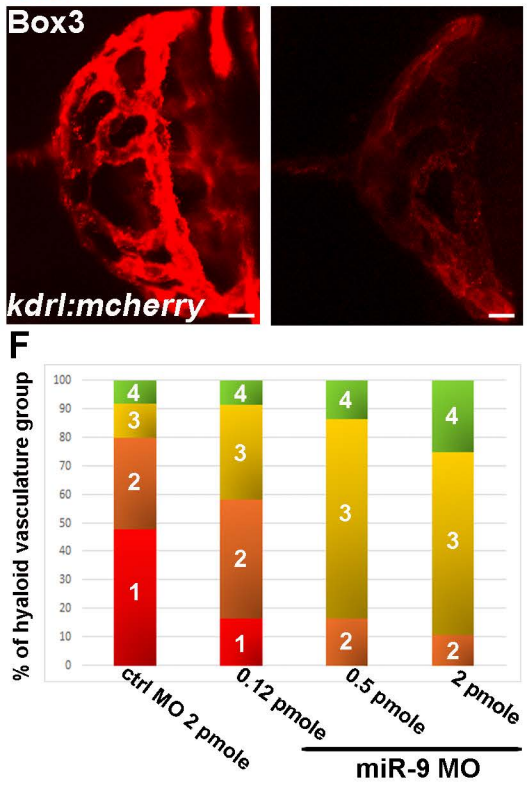
F
% of hyaloid vasculature group
100
90
80
70
60
50
40
30
20
10
0
ctrl MO 2 pmole
0.12 pmole
0.5 pmole
2 pmole
miR-9 MO

Figure S3

Supplemental Figure 3: miR-9 controls the neurovasculature formation in a dose dependent manner (related to Figure 2)

(A) Schematic representation of the miR-9 MO binding to microRNA-9. With the control MO, miR-9 is available, allowing the degradation of the mRNA target and revealing the *miR-9* expression pattern with the specific miR-9 LNA probe. In presence of the miR-9 MO, miR-9 is bound by the MO, inhibiting the mRNA degradation and the binding of the LNA probe. **(B)** Whole-mount in situ hybridization against miR-9 at 72 hpf shows that miR-9 knockdown does not affect trunk morphogenesis.mCherry immunolabelling in *Tg(kdrl:mCherry)* at 72 hpf showing blood vessels formation in the trunk of control or miR-9 morphant larvae. In the trunk, miR-9 knockdown does not affect blood vessels development. **(C)** Confocal projections of mCherry immunolabelling in *Tg(kdrl:mCherry)* at 72 hpf showing blood vessels formation in control or miR-9 morphant larvae in the brain. The affected neurovasculature in the midbrain, hindbrain and retina is highlighted by an asterisk. (**D, E**) Whole-mount in situ hybridization against *miR-9* at 72 hpf in larvae injected with the control MO or the miR-9 MO in the retina (D) and brain (E). Confocal projections of mCherry immunolabelling in *Tg(kdrl:mCherry)* at 72 hpf showing blood vessels formation in control MO and miR-9 MO injected larvae. Higher is the quantity of miR-9 MO injected in the egg, stronger is inhibition of *miR-9* expression. The severity of the neurovasculature defects is correlated to the level of miR-9 inhibition. (**F**) The formation of the hyaloid vasculature in the retina of control MO (n=25) or miR-9 MO dilution series (n=24, 30 and 28 for croissant dilutions respectively) at 72 hpf was classified in four groups and quantified. Group 1: The blood vessels form a complex vascular network. Group 2: The hyaloid vasculature shows a reduced branching complexity. Group 3: In addition to the reduction of the branching, the caliber is affected and some vessels appear to be thicker. Group 4: The hyaloid vasculature is absent. Dorsal view of the brain with anterior up. Lateral view of the retina. Box1 is a close up of the retina. Box2 is a close up of the hindbrain. Box3 is a close up of the hyaloid vasculature in the retina. Scale bars: 10 µm for immunolabelling and 100 µm for whole mount ISH.

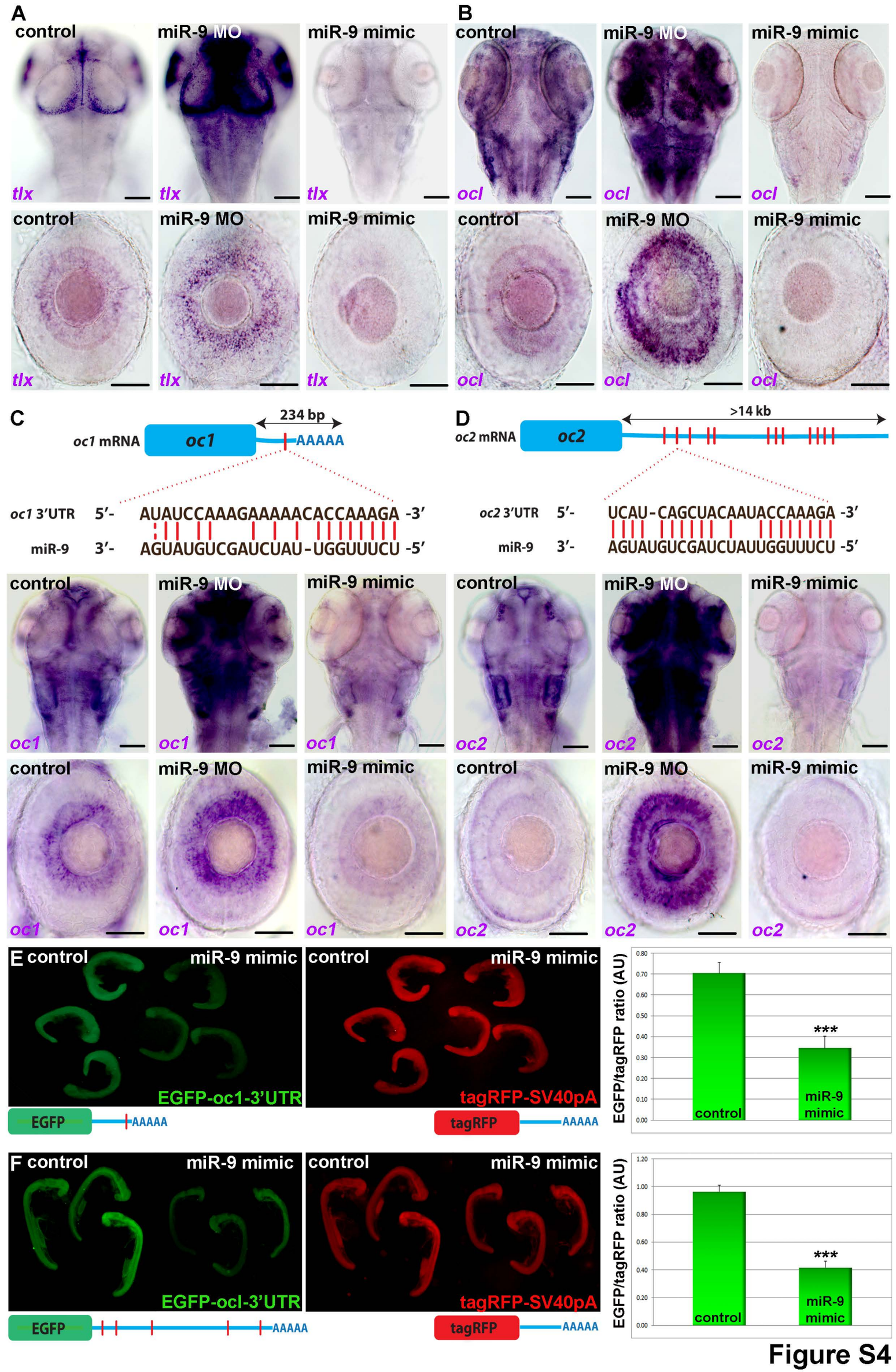
A
control
miR-9 MO
miR-9 mimic
tlx
B
ocl
C
234 bp
oc1 mRNA
oc1
AAAAA
oc1 3'UTR 5'- AUAUCCAAAGAAAAACACCAAAGA -3'
miR-9 3'- AGUAUGUCGAUCUAU-UGGUUUCU -5'
D
>14 kb
oc2 mRNA
oc2
oc2 3'UTR 5'- UCAU-CAGCUACAAUACCAAAGA -3'
miR-9 3'- AGUAUGUCGAUCUAUUGGUUUCU -5'
oc1
oc2
E control
miR-9 mimic
EGFP-oc1-3'UTR
tagRFP-SV40pA
EGFP
tagRFP
AAAAA
EGFP/tagRFP ratio (AU)
***
F
EGFP-ocl-3'UTR

Figure S4

Supplemental Figure 4: Validation of miR-9 targets conserved across vertebrates (related to Figure 3)

(A, B) Whole-mount in situ hybridization against *tlx* (A) or *ocl* (B) in larvae at 72 hpf injected with the control MO, the miR-9 MO or the miR-9 RNA mimic. *tlx* and *ocl* behave like a miR-9 target showing an increase in the miR-9 knockdown and a decrease in the miR-9 gain of function. **(C, D)** Schematic representation of the zebrafish *oc1* (C) and *oc2* (D) mRNA indicating the sequence of the putative miR-9 binding sites in the 3'UTR (red). Whole-mount in situ hybridization against *oc1* (C) and *oc2* (D) in larvae at 72 hpf injected with the control MO, the miR-9 MO or the miR-9 RNA mimic. *onecut* family mRNAs behave like miR-9 targets showing an increase in the miR-9 knockdown and a decrease in the miR-9 gain of function. (**E, F**) Fluorescent sensor assay to test the functionality of miR-9 binding sites in the 3'UTR of *oc1* (E) and *ocl* (F) showing that miR-9 mediates *oc1* and *ocl* inhibition via the 3'UTR. TagRFP and EGFP protein expression in embryos at 24 hpf: embryos were co-injected with the *egfp* mRNA containing the 3'UTR of *oc1* (n=7) or *ocl* (n=3) fused to the SV40pA and the internal control, *tagrfp* mRNA (n=8 and 3 respectively) in the presence or absence of miR-9 mimic. The ratio between the level of EGFP and TagRFP proteins fluorescence shows a decrease in EGFP expression, but not TagRFP, in the presence of the miR-9 RNA mimic. Dorsal view of the brain with anterior up. Lateral view of the retina. Scale bars: 100 μm. Error bars represent s.d. **P*<0.05, ***P*<0.001, ****P*<0.0005, determined by *t*-test, two-tailed.

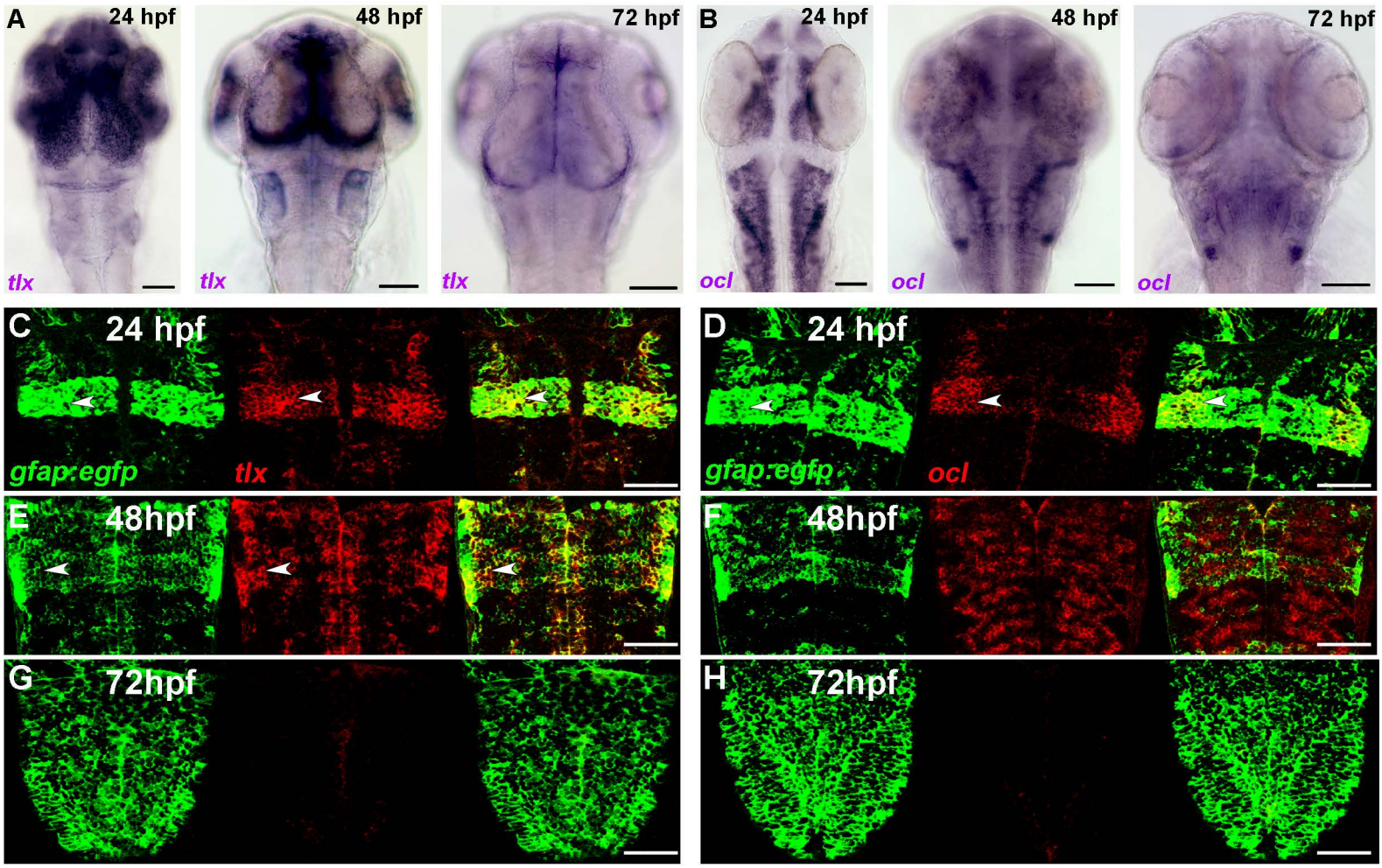
A
24 hpf
48 hpf
72 hpf
tlx
tlx
tlx
B
24 hpf
48 hpf
72 hpf
ocl
ocl
ocl
C
24 hpf
gfap:egfp
tlx
D
24 hpf
gfap:egfp
ocl
E
48hpf
F
48hpf
G
72hpf
H
72hpf

Figure S5

Supplemental Figure 5: Neural expression of *tlx* and *ocl* (related to Figure 3)

(A, B) Whole-mount in situ hybridization showing the time course of *tlx* (A) and *ocl* (B) expression in the developing embryo at 24, 48 and 72 hpf. During development, when *miR-9* expression becomes broader and stronger after 24 hpf, we observe a correlative decrease in *tlx* and *ocl* expression. (**C-H**) Confocal section of double in situ/immunolabelling with *tlx* or *ocl* mRNAs and EGFP in the *Tg(gfap:gal4); Tg(uas:egfp)* line labelling NSCs in the hindbrain. When miR-9 is not expressed broadly throughout the brain at 24 hpf, we observed an overlap in the expression of *tlx* and *ocl* with the NSCs marker GFAP (C, D). At 48 hpf, when miR-9 is strongly expressed in the brain *ocl* is excluded from the NSCs domain (E, F). At 72 hpf, both *tlx* and *ocl* are not detected in NSCs (G, H). Arrowheads show co-localization with EGFP. Dorsal view of the brain with anterior up. Scale bars: 100 µm.

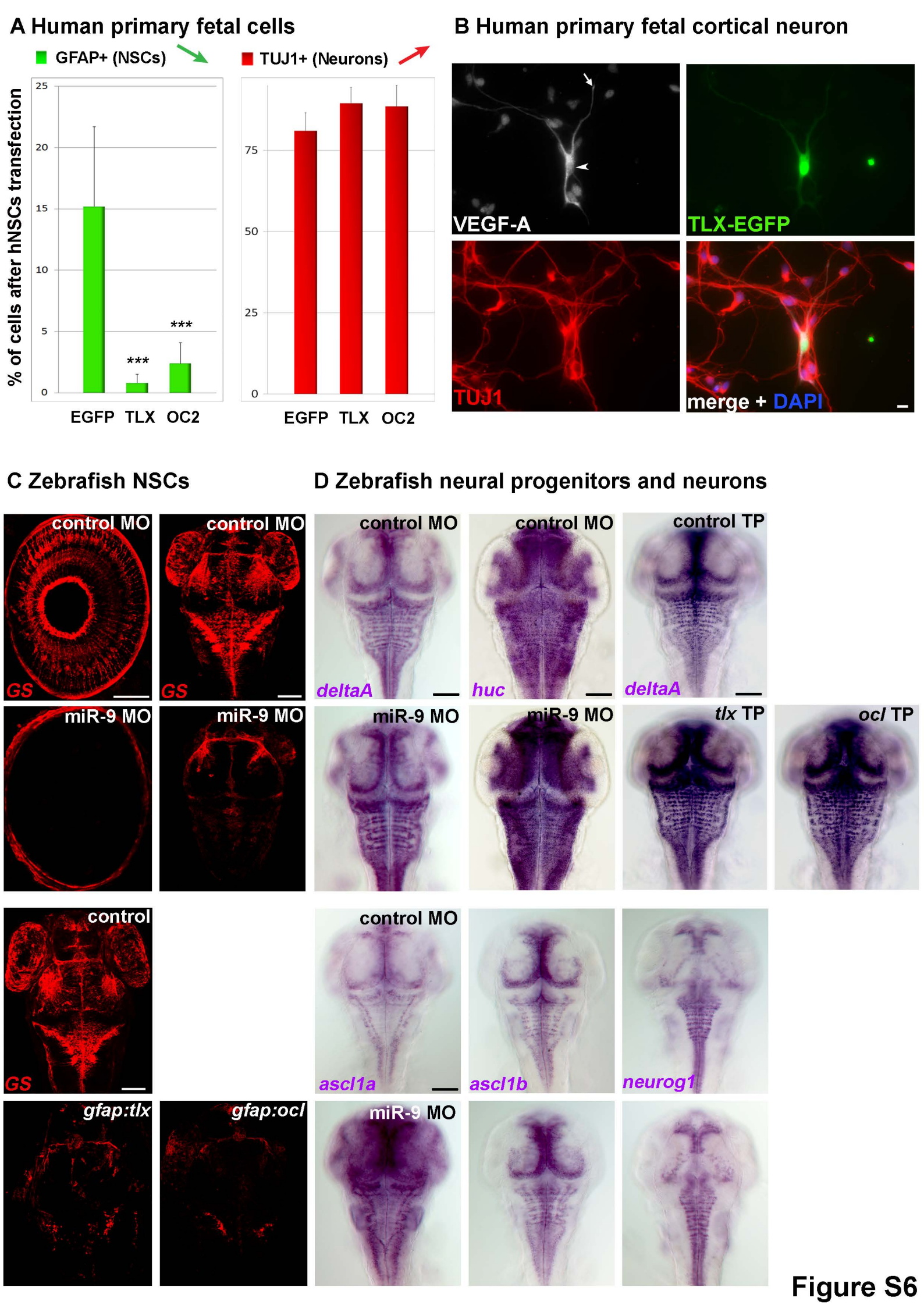
A Human primary fetal cells
GFAP+ (NSCs)
TUJ1+ (Neurons)
% of cells after hNSCs transfection
25
20
15
10
5
0
***
***
EGFP TLX OC2
75
50
25
0
EGFP TLX OC2
B Human primary fetal cortical neuron
VEGF-A
TLX-EGFP
TUJ1
merge + DAPI
C Zebrafish NSCs
control MO
control MO
GS
GS
miR-9 MO
miR-9 MO
control
GS
gfap:tlx
gfap:ocl
D Zebrafish neural progenitors and neurons
control MO
control MO
control TP
deltaA
huc
deltaA
miR-9 MO
miR-9 MO
tlx TP
ocl TP
control MO
ascl1a
ascl1b
neurog1
miR-9 MO

Figure S6

Supplemental Figure 6: TLX and OC activity control neural stem cells fate (related to Figure 4)

(A) *In vitro* effect of transfecting primary human embryonic neural stem cells with a control EGFP plasmid, TLX-p2A-EGFP or OC2-p2A-EGFP. Overexpression of TLX (n=646) and OC2 (n=528) significantly depletes the existing neural stem cell population in the dish compared to the EGFP control (n=408). Furthermore, in comparison with EGFP transfection (n=344), expression of TLX (n=99) and OC2 (n=69) slightly increases the percentage of primary human NSCs that differentiate into cortical neurons. **(B)** Triple immunolabelling against TUJ1, EGFP and VEGF-A after transfection of primary human embryonic NSCs with the TLX-p2A-EGFP plasmid (nuclear marker DAPI is in blue). Embryonic cortical neuron express high detectable level of nuclear (arrowhead) and cytoplasmic (arrow) VEGF-A after TLX expression (EGFP). **(C)** Confocal projection of immunolabelling with endogenous GS protein in the brain of control MO or miR-9 MO injected larvae and larvae expressing *uas:tlx* or *uas:ocl* in NSCs using *Tg(gfap:gal4)* line at 72 hpf. Embryonic NSCs are reduced in the miR-9 depleted and *tlx* or *ocl* expressing brain. **(D)** Whole-mount in situ hybridization against *deltaA*, *ascl1a*, a*scl1b*, *neurog1* or *huc* in embryos at 48 hpf injected with the control MO, miR-9 MO*, tlx* TP or *ocl* TP. miR-9 inhibition increases neural progenitor cells (*deltaA* and *ascl1a*) and promote a neuronal fate (*huc*). *tlx* or *ocl* mRNA protection also leads to an increase in *deltaA*+ neural progenitors in the zebrafish brain. Of note, miR-9 morphant shows an increase in *deltaA*+ and *ascl1a*+ NPCs but not *ascl1b*+ or *neurog*1+ NPCs. Dorsal view, Anterior up. Scale bars: 10 µm (B) or 100 µm (C, D). Error bars represent s.d. **P*<0.05, ***P*<0.001, ****P*<0.0005, determined by *t*-test, two-tailed.

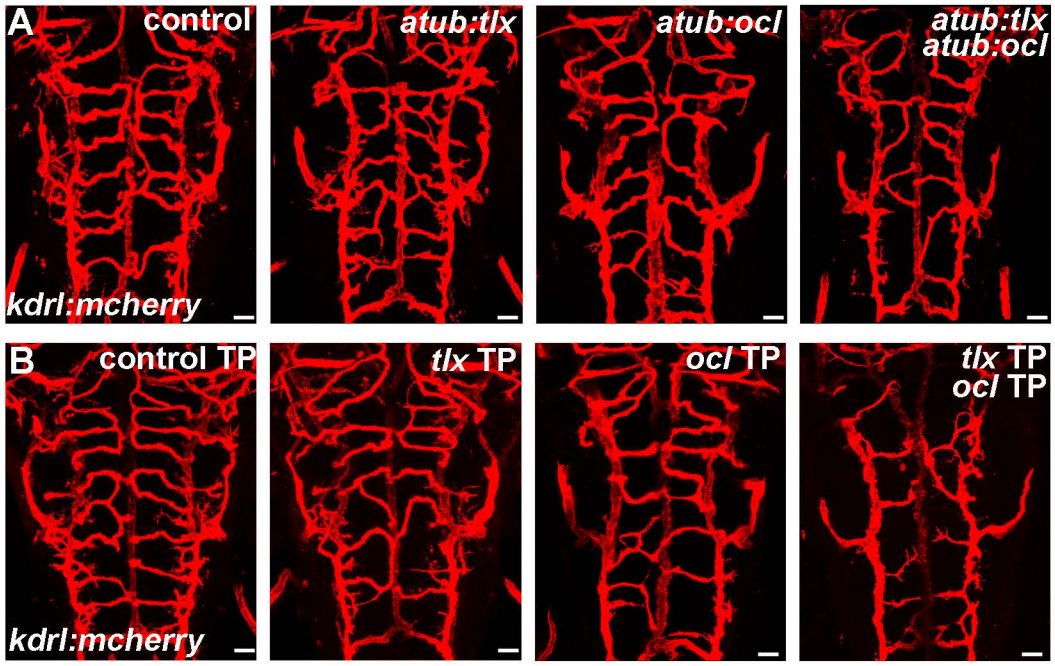
A
control
atub:tlx
atub:ocl
atub:tlx
atub:ocl
kdrl:mcherry
B
control TP
tlx TP
ocl TP
tlx TP
ocl TP
kdrl:mcherry

Figure S7

Supplemental Figure 7: Tlx and Ocl neuronal expression affect vasculature development (related to Figure 4)

(A) Confocal projections of mCherry immunolabelling in *Tg(kdrl:mCherry)* at 72 hpf showing blood vessels formation in the hindbrain of controls or larvae expressing *uas:tlx*, *uas:ocl* or *uas:tlx* and *uas:ocl* in a pan-neuronal manner in *Tg(alpha-tubulin:gal4)* line. **(B)** Confocal projections of mCherry immunolabelling in *Tg(kdrl:mCherry)* at 72 hpf showing blood vessels formation in the hindbrain of control MO, *tlx* TP, *ocl* TP or *tlx* and *ocl* TP larvae**.** Dorsal view of the brain with anterior up. Scale bars: 10 µm.

SUPPLEMENTAL EXPERIMENTAL PROCEDURES

Primary human embryonic neural stem cells culture, purification and transfection

Human fetal cortex was collected after elective abortion by a commercial vendor (StemExpress, Placervill, CA). The meninges were removed and the tissue was enzymatically dissociated to make a suspension of single cells as described previously (Cahoy et al., 2008; Dugas et al., 2006). Briefly, the tissue was incubated at 33°C for 45 minutes in 20 ml of a papain solution containing Earle's balanced salts (EBSS, Sigma, St. Louis, MO, E7510), D(+)-glucose (22.5mM), NaHCO3 (26mM), DNase (125U/ml, Worthington, Lakewood, NJ, LS002007), papain (4 U/ml, Worthington, Lakewood, NJ, LS03126), and L-cysteine (1mM, Sigma, St. Louis, MO, C7880). The papain solution was equilibrated with 5% CO2 and 95% O2 gas before and during papain treatment. Following papain treatment, the tissue was washed three times with 4.5ml of inhibitor buffer containing BSA (1.0mg/ml, Sigma, St. Louis, MO, A-8806), and ovomucoid (also known as trypsin inhibitor, 1.0 mg/ml, Roche Diagnostics Corporation, Indianapolis, IN 109878) and then mechanically dissociated by gentle sequential trituration using a 5ml pipette. Dissociated cells were layered on top of 10ml of high concentration inhibitor solution with 5mg/ml BSA and 5mg/ml ovomucoid and centrifuged at 130g for 5 minutes. The cell pellet was then resuspended in 12 ml Dulbecco's phosphate-buffered saline (DPBS, Invitrogen, Carlsbad, CA 14287) containing 0.02% BSA and 12.5U/ml DNase and filtered through a 20um Nitex mesh (Sefar America Inc., Depew NY, Lab Pak 03-20/14) to remove undissociated cell clumps. Cell health was assessed by trypan blue exclusion.

To purify neural stem cells, the single cell suspension was immunopanned with a CD15 antibody (BD, mouse) for a 30 minute incubation. The adherent cells on the CD15 plate were washed 8 times with 10-20 ml of DPBS to remove all antigen-negative nonadherent cells, and then removed from the plate by treating with trypsin (Sigma, 1,000U/ml, T-4665) in 8ml Ca^{2+} and Mg^{2+} free EBSS (Irvine Scientific, Santa Ana, CA, 9208) for 3-10 minutes at 37°C in a 10% CO2 incubator. The cells were dislodged by gentle squirting of over the plate and harvested by centrifugation at 200g for 10 minutes.

Plasmid transfection was performed on purified neural stem cells from 14 week-old human fetal brains. TLX and ONECUT2 ORF were amplified by PCR from human cDNA, fused to the p2A-EGFP and cloned in the pCDNA3.1 vector downstream of a CMV promoter. EGFP, TLX, and OC2 plasmids were transfected into cells using the nucleofector kit (Lonza) for primary neural stem cells. 2-4ug of each plasmid was added to the cell suspension and briefly electoporated according to the user protocol. Cells were then plated on PDL coated coverslips and cultured in a defined media including DMEM, insulin, pyruvate, Pen/Strep, L-glutamine, Sato, and N-acetylcysteine. Two 14 week-old brains were used to prepare 6 samples for each condition, each sample containing 150-450 cells.

Generation of human iPSC-derived cortical neurons

Human iPSCs derived from healthy individuals were grown on inactivated mouse embryonic fibroblasts feeders in iPSC medium (DMEM/F12, 20% Knockout Serum, 1mM non-essential amino acids, GlutaMax (1:200),

0.1mM β-mercaptoethanol, penicillin and streptomycin (1:100)). Colonies of iPSCs were detached with dispase (0.35mg/ml, Invitrogen) and transferred into low-attachment plates in iPSC medium supplemented with dorsomorphin (5 µM, Sigma) and SB-431542 (10 µM, Tocris), and the medium was changed daily. On day six of *in vitro* differentiation, neural spheroids were transferred to neural medium (NM) (Neurobasal A, B27 without vitamin A, GlutaMax (1:100), penicillin and streptomycin (1:100); Life Technologies), which was supplemented with EGF (20 ng/ml) and FGF2 (20 ng/ml) until day 24, and then supplemented with BDNF (20 ng/ml) and NT3 (20 ng/ml) from day 25 to 42. From day 43 onwards, cortical spheroids were maintained in NPC with medium changes every 4 days.

For enzymatic dissociation and culture in monolayer (Deverman et al., 2016), hCS were incubated with accutase for 15 minutes at 37°C, washed 3 times with NM and gently triturated with a P-200 pipet. Cells were plated on poly-ornithine and laminin coated glass coverslips (15 mm) at around 300,000 cells/well and maintained in NM supplemented with BDNF (20 ng/ml) and NT3 (20 ng/ml) with half medium changes every other day.

Zebrafish transgenic lines and plasmid construction

The following transgenic lines were used to visualize: post-mitotic neurons *Tg(huc:egfp)* (Park et al., 2000), neural stem cells *Tg(gfap:gal4); Tg(uas:egfp), miR-9* expressing cells *Tg(CNE1:egfp),* referred as *Tg(hsa-MIR-9-2:egfp)* or endothelial cells *Tg(kdrl:ras-mCherry*) (Chi et al., 2008) and *Tg(kdrl:egfp*) (Choi et al., 2007a).

For the generation of *Tg(alpha-tubulin:gal4)* and *Tg(gfap:gal4)*, the goldfish *a1-tubulin* promoter (Hieber et al., 1998) and the zebrafish *gfap* promoter (Bernardos and Raymond, 2006) were cloned into the p5E 5' entry vector of the tol2kit (Kwan et al., 2007). Then, the 5' entry vector was recombined into the Tol2 transposon destination vector. *pTol2-vegfaa:egfp* was by made by PCR amplification of 1.5kb upstream of the *vegfaa* promoter from zebrafish genomic DNA. PCR products were directionally cloned into the XhoI and BglII sites of the pTol2-E1b:EGFP vector. To establish *Tg(alpha-tubulin:gal4), Tg(gfap:gal4) and Tg(*CNE1*:egfp)* stable transgenic lines, plasmids were injected into one-cell stage embryos with the Tol2 mRNA transposase (Kwan et al., 2007).

To generate *pDestTol2-uas:vegfaa*, *pDestTol2-uas:tlx*, *pDestTol2-uas:ocl*, *pDestTol2-uas:tlx-p2A-egfp*, *pDestTol2-uas:ocl-p2a-egfp pDestTol2-hs:tlx*, *pDestTol2-hs:ocl*, *pDestTol2-hs:tlx-p2A-egfp* and *pDestTol2-hs:ocl-p2A-egfp* plasmids for transient expression; *vegfaa*, *tlx* and *ocl* ORF were amplified by PCR from zebrafish cDNA and cloned in the pME entry vector of the tol2kit. The appropriate middle entry clone was mixed with the UAS or the heat-shock promoter 5' entry vector and the SV40pA 3' entry vector, and recombined into the Tol2 transposon destination vector (Kwan et al., 2007).

I*n situ* hybridization

In situ hybridizations were performed as previously described (Oxtoby and Jowett, 1993). Previously described antisense DIG labelled probes for *neurog1* (Blader et al., 1997), *deltaA* (Haddon et al., 1998), *ascl1a* and *ascl1b* (Allende and Weinberg, 1994) were generated using standard procedures. ORFs were cloned in a pCS2+ vector using zebrafish cDNA for *vegfaa, tlx, oc1, oc2,* and *ocl* or human cDNA for *SOX2*; and antisense DIG

labelled probes were transcribed using the linearized pCS2+ plasmid containing the ORF. For miR-9 ISH, the previously described miRCURY detection probe (LNA) hsa–miR-9 (Exiqon) was used (Leucht et al., 2008). *In situs* were revealed using either BCIP and NBT (Roche) or Fast Red (Roche) as substrates.

Antisense morpholino and microRNA-9 mimic injection

We used the previously described miR-9 MO (TCATACAGCTAGATAACCAAAGA) and the control MO (CACCAAACCATATAGAAGTGATA) (Leucht et al., 2008). Embryos were injected at the one-cell stage with 0.12 to 2 pmole of the miR-9 or control MO. *tlx* (GCTTGCTCATATTGAAGACCACGGC) and *ocl* (ACATCTCTCCCATATTACCATCCAT) MOs were injected at 1 pmole and the efficiency of the MO was tested by the capacity of the MO to down-regulate EGFP (but not the internal mCherry control) expression driven by a construct containing the MO binding site in the 5'UTR of *tlx* or *ocl* fused to a p2A-EGFP (data not shown). For target protection, *tlx* TP (CCTTTGGTTTTCAGCACTATGTCAA), *ocl* TP (TCTTTGGTATTGGGACTCCTATCAG), and control TP (CTGTGGCCTAAAGGGTCTAGACATG) were designed as previously described (Choi et al., 2007b; Staton and Giraldez, 2011) and used at 1 pmole.

Gain of function of miR-9 was performed with the injection of the *mirVana* miR-9 RNA mimic, hsa-miR-9-5 (2 µM, Ambion).

Mosaic analysis

For mosaic expression of *uas:vegfaa*, *uas:tlx*, *uas:ocl*, *uas:tlx-p2A-egfp*, *uas:ocl-p2A-egfp*, *hs:tlx*, *hs:ocl*, *hs:tlx-p2A-egfp* and *hs:ocl-p2A-egfp,* the appropriate Tol2 based construct (25 ng/µl) was co-injected with synthetic mRNA encoding the Tol2 transposase (25ng/µl) into one-cell stage embryos. Heat-shocks were performed in a water bath at 37°C for 1 hour. For pan-neuronal expression using the *uas* promoter, the injection was performed in embryos from crosses between identified heterozygote carriers of *Tg(alpha-tubulin:gal4)* and *Tg(kdrl:ras-mCherry)*. Expression in neural stem cells was performed by injection in the *Tg(gfap:gal4)* line.

Drug treatments

Tg(*kdrl:ras-mCherry*) embryos were treated with 0.06 µM solution of the chemical tyrosine kinase inhibitor SU5416 (S8442, Sigma Aldrich) dissolved in DMSO (Herbert et al., 2009). Treatments started at 30 hpf and both DMSO and SU5416 treated embyos were fixed at 72 hpf to quantify the blood vessels sprouting.

Fluorescent sensor assay

Fluorescent sensor assay with the 3'UTR of *oc1* and *ocl* was performed as described in (Staton and Giraldez, 2011). Capped mRNAs for EGFP containing the *oc1* or *ocl* 3'UTR and TagRFP reporter constructs were synthetized using linearized pCS2+ plasmids and mMessage mMachine kit (Ambion). Zebrafish embryos were injected at a one-cell stage with 150ng/µL of EGFP and TagRFP mRNAs and either a control or miR-9 RNA mimics (2 µM, Ambion). The ratio of EGFP/TagRFP fluorescence was quantified using ImageJ software.

In silico predictions

Putative targets for miR-9 in human were first searched using the ElMMo miRNA target prediction server (http://www.mirz.unibas.ch/ElMMo3). 3'UTR of orthologous genes in zebrafish were retrieved from the Ensembl web server and searched for conserved miR-9 binding sites (Bartel, 2009).

The miR-9 consensus binding sequence (Leucht et al., 2008) was queried against the 3'UTR of each human gene in the GRCh37 human reference (hg19) using LASTZ (version 1.02.00) with sensitive parameters (--hspthresh=500 --gappedthresh=500 --seed=match6). The highest scoring alignments from LASTZ were inspected for conservation using the UCSC 46-way multiple alignment (Karolchik et al., 2014).

SUPPLEMENTAL REFERENCES

Allende, M.L., and Weinberg, E.S. (1994). The expression pattern of two zebrafish achaete-scute homolog (ash) genes is altered in the embryonic brain of the cyclops mutant. Developmental biology *166*, 509-530.

Bartel, D.P. (2009). MicroRNAs: target recognition and regulatory functions. Cell *136*, 215-233.

Bernardos, R.L., and Raymond, P.A. (2006). GFAP transgenic zebrafish. Gene expression patterns : GEP *6*, 1007-1013.

Blader, P., Fischer, N., Gradwohl, G., Guillemot, F., and Strahle, U. (1997). The activity of neurogenin1 is controlled by local cues in the zebrafish embryo. Development *124*, 4557-4569.

Cahoy, J.D., Emery, B., Kaushal, A., Foo, L.C., Zamanian, J.L., Christopherson, K.S., Xing, Y., Lubischer, J.L., Krieg, P.A., Krupenko, S.A*., et al.* (2008). A transcriptome database for astrocytes, neurons, and oligodendrocytes: a new resource for understanding brain development and function. The Journal of neuroscience : the official journal of the Society for Neuroscience *28*, 264-278.

Chi, N.C., Shaw, R.M., De Val, S., Kang, G., Jan, L.Y., Black, B.L., and Stainier, D.Y. (2008). Foxn4 directly regulates tbx2b expression and atrioventricular canal formation. Genes & development *22*, 734-739.

Choi, J., Dong, L., Ahn, J., Dao, D., Hammerschmidt, M., and Chen, J.N. (2007a). FoxH1 negatively modulates flk1 gene expression and vascular formation in zebrafish. Developmental biology *304*, 735-744.

Choi, W.Y., Giraldez, A.J., and Schier, A.F. (2007b). Target protectors reveal dampening and balancing of Nodal agonist and antagonist by miR-430. Science *318*, 271-274.

Deverman, B.E., Pravdo, P.L., Simpson, B.P., Kumar, S.R., Chan, K.Y., Banerjee, A., Wu, W.L., Yang, B., Huber, N., Pasca, S.P*., et al.* (2016). Cre-dependent selection yields AAV variants for widespread gene transfer to the adult brain. Nature biotechnology *34*, 204-209.

Dugas, J.C., Tai, Y.C., Speed, T.P., Ngai, J., and Barres, B.A. (2006). Functional genomic analysis of oligodendrocyte differentiation. The Journal of neuroscience : the official journal of the Society for Neuroscience *26*, 10967-10983.

Haddon, C., Smithers, L., Schneider-Maunoury, S., Coche, T., Henrique, D., and Lewis, J. (1998). Multiple delta genes and lateral inhibition in zebrafish primary neurogenesis. Development *125*, 359-370.

Herbert, S.P., Huisken, J., Kim, T.N., Feldman, M.E., Houseman, B.T., Wang, R.A., Shokat, K.M., and Stainier, D.Y. (2009). Arterial-venous segregation by selective cell sprouting: an alternative mode of blood vessel formation. Science *326*, 294-298.

Hieber, V., Dai, X., Foreman, M., and Goldman, D. (1998). Induction of alpha1-tubulin gene expression during development and regeneration of the fish central nervous system. Journal of neurobiology *37*, 429-440.

Karolchik, D., Barber, G.P., Casper, J., Clawson, H., Cline, M.S., Diekhans, M., Dreszer, T.R., Fujita, P.A., Guruvadoo, L., Haeussler, M*., et al.* (2014). The UCSC Genome Browser database: 2014 update. Nucleic acids research *42*, D764-770.

Kwan, K.M., Fujimoto, E., Grabher, C., Mangum, B.D., Hardy, M.E., Campbell, D.S., Parant, J.M., Yost, H.J., Kanki, J.P., and Chien, C.B. (2007). The Tol2kit: a multisite gateway-based construction kit for Tol2 transposon transgenesis constructs. Developmental dynamics : an official publication of the American Association of Anatomists *236*, 3088-3099.

Leucht, C., Stigloher, C., Wizenmann, A., Klafke, R., Folchert, A., and Bally-Cuif, L. (2008). MicroRNA-9 directs late organizer activity of the midbrain-hindbrain boundary. Nature neuroscience *11*, 641-648.
Oxtoby, E., and Jowett, T. (1993). Cloning of the zebrafish krox-20 gene (krx-20) and its expression during hindbrain development. Nucleic acids research *21*, 1087-1095.
Park, H.C., Kim, C.H., Bae, Y.K., Yeo, S.Y., Kim, S.H., Hong, S.K., Shin, J., Yoo, K.W., Hibi, M., Hirano, T.*, et al.* (2000). Analysis of upstream elements in the HuC promoter leads to the establishment of transgenic zebrafish with fluorescent neurons. Developmental biology *227*, 279-293.
Staton, A.A., and Giraldez, A.J. (2011). Use of target protector morpholinos to analyze the physiological roles of specific miRNA-mRNA pairs in vivo. Nature protocols *6*, 2035-2049.